

Supplementary Information

Tuning the liquid crystal behavior of Subphthalocyanines: effects of substitution, chirality, and hydrogen bonding

Jorge Labella,^{*a,b} Elisa López-Serrano,^a Jorge Labrador-Santiago,^a Joaquín Barberá,^{c,d} César L. Folcia,^e Teresa Sierra^{*c,d} and Tomás Torres ^{*a,f,g}

- [a] Department of Organic Chemistry, Universidad Autónoma de Madrid, Campus de Cantoblanco. C/ Francisco Tomás y Valiente 7, 28049 Madrid (Spain)
- [b] Department of Molecular Engineering, Kyoto University Katsura, Kyoto 615-8510, Japan.
- [c] Instituto de Nanociencia y Materiales de Aragón (INMA), CSIC-Universidad de Zaragoza, 50009 Zaragoza, Spain. E-mail: tsierra@unizar.es
- [d] Departamento de Química Orgánica, Facultad de Ciencias, Universidad de Zaragoza, 50009 Zaragoza, Spain.
- [e] Department of Physics, Faculty of Science and Technology, UPV/EHU, 48940 Bilbao, Spain.
- [f] Institute for Advanced Research in Chemical Sciences (IAdChem), Universidad Autónoma de Madrid, Madrid (Spain).
- [g] IMDEA – Nanociencia C/ Faraday 9, Campus de Cantoblanco, 28049 Madrid (Spain)

Table of contents

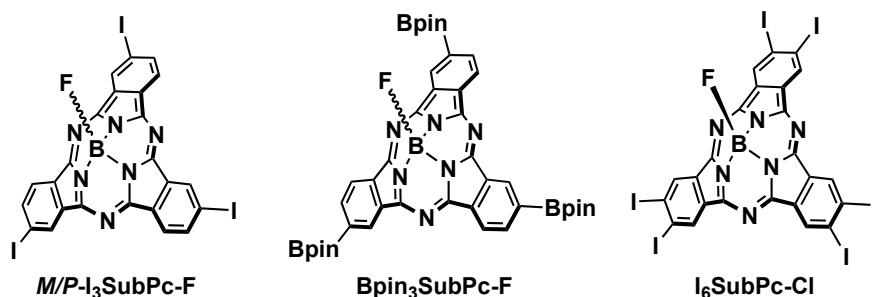
| | |
|--|----|
| 1. Materials and methods..... | 2 |
| 2. Synthetic procedures and compound data..... | 2 |
| 3. Additional liquid crystal characterization..... | 8 |
| 4. Theoretical calculations details..... | 15 |
| 5. References..... | 15 |

1. Materials and methods

The monitoring of the reactions has been carried out by thin layer chromatography (TLC), employing aluminum sheets coated with silica gel type 60 F254 (0.2 mm thick, Merck). The analysis of the TLCs was carried out with an UV lamp of 254 and 365 nm. Purification and separation of the synthesized products were performed by normal-phase column chromatography, using silica-gel (230–400 mesh, 0.040–0.063 mm, Merck). Eluents along with the relative ratio in the case of solvent mixtures are indicated for each particular case. Nuclear magnetic resonance spectra (^1H -, ^{13}C -, ^{11}B -, ^{19}F -NMR) were recorded on a Bruker AV-300, Bruker AV III HD 400 MHz or Bruker DRX-500 spectrometers. Deuterated solvent employed in each case is indicated in brackets, and its residual peak was used to calibrate the spectra using literature reference δ ppm values.¹ All the experiments were recorded at room temperature. High-resolution mass spectra (HRMS) were recorded in the Interdepartmental Investigation Service of UAM employing matrix-assisted laser desorption/ionization time-of-flight (MALDI-TOF) using a Bruker-Ultraflex-III spectrometer with a Nd:YAG laser operating at 355 nm or ultrafleXtreme spectrometer. The matrixes and internal references employed are indicated for each spectrum. Ultraviolet and visible (UV-Vis) spectra were recorded using solvents in the spectroscopic grade in the Organic Chemistry Department of UAM employing JASCO-V660 and PerkinElmer Lambda 2 dual beam absorption spectrophotometers. The logarithm of the molar extinction coefficient (ϵ) is indicated in brackets for each maximum. Dry solvents were purchased from commercial suppliers in anhydrous grade or thoroughly dried before use employing standard methods. Solid, hygroscopic reagents were dried in a vacuum oven before use.

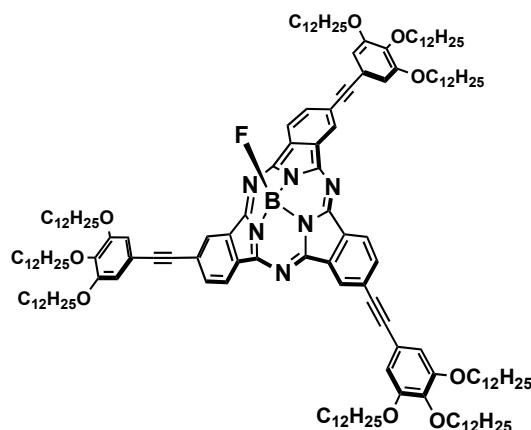
2. Synthetic procedures and compound data

The synthesis and characterization of **5-bromo-1,2,3-tris(dodecyloxy)benzene** and **SubPcs 1**,² **4**,³ **M/P-I₃SubPc-F**,³ **I₆SubPc-Cl**,⁴ and **Bpin₃SubPc-F**⁵ have been previously reported.

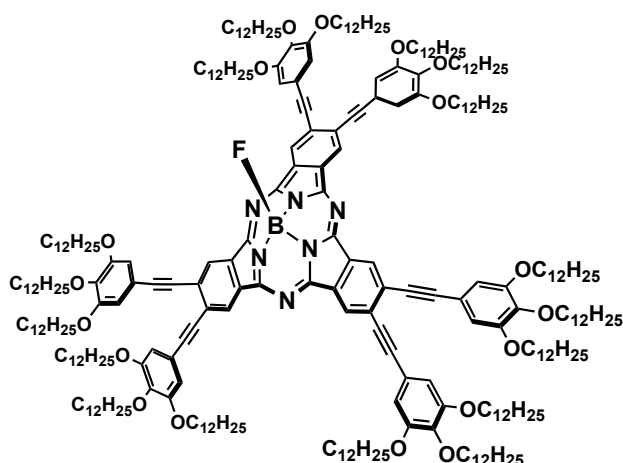


Synthesis and characterization of SubPcs

SubPc 1M/P



As discussed in the manuscript, this compound was synthesized via post-functionalization of *M/P*-**I₃SubPc-F**, following the procedure previously reported in our group for preparing the racemic version.³ The characterization data of *M/P*-**A₃SubPc-F** are identical to those reported for *RAC*-**A₃SubPc-F**.



SubPc 2

In a 25 mL Schlenk flask, equipped with a magnetic stirrer, **I₆SubPc-Cl** (30 mg, 0.026 mmol), PdCl₂(PPh₃)₂ (7.2 mg, 0.001 mmol), CuI (3.9 mg, 0.0021 mmol), and 3,4,5-tri(dodecyloxy)phenylacetylene (121 mg, 0.19 mmol) were placed under argon atmosphere. Then, 4.5 mL of a mixture of THF/NEt₃ 5:1, which was deoxygenated via three freeze-pump-thaw cycles, was added and the resulting mixture was stirred at 50 °C for 30 min, and then at rt overnight. After that, the crude was dissolved in DCM and passed through a short celite plug. The solvent was removed by vacuum distillation and the resulting dark green solid was purified by column chromatography on silica gel using DCM/heptane 2:1 as eluent. 30 mg of the resulting axially chlorinated SubPc (0.07 mmol) was placed in a 10 mL Schlenk flask equipped with a magnetic stirrer. Then, silver tetrafluoroborate (25 mg, 0.13 mmol) and 1 mL of dry toluene were added, and the mixture was stirred at rt for 12 h. The solvent was then eliminated under reduced pressure and the residue was purified by column chromatography on silica gel (eluent: DCM/hexane 2:1) and by size exclusion chromatography using Bio-Beads (eluent: CHCl₃). Upon recrystallization from methanol, **SubPc 2** was obtained as a green solid (28 mg, 0.07 mmol). Overall yield: 60%.

Mp = 23–28 °C; **¹H-NMR** (300 MHz, CDCl₃): δ (ppm) = 8.98 (s, 6H), 6.84 (s, 12H), 4.05 (t, *J* = 3.6 Hz, 12H), 3.88 (t, *J* = 3.6 Hz, 24H), 1.77 (m, 46H), 1.48–1.40 (m, 314H), 0.87 (t, *J* = 5.2 Hz, 54H); **¹³C-NMR** (75.5 MHz, CDCl₃): Due to the high molecular weight and the limited solubility of this molecule, the acquisition of this spectrum was not possible; **¹¹B-NMR** (160.5 MHz, CDCl₃): δ (ppm) = –13.6 (d, *J* = 32.1 Hz, 1B; B–F); **¹⁹F-NMR** (470 MHz, CDCl₃): δ (ppm) = –156.0 (q, *J* = 32.9 Hz, 1F; B–F); **MS** (MALDI-TOF, DCTB): *m/z* = 4332.4 [M]⁺; **HRLSI-MS** (DCTB + PPGNa 5000): *m/z* Calculated for [C₂₈₈H₄₆₈BFN₆O₁₈]: 4332.6074, Found: 4332.5948; **UV-vis** (CHCl₃): λ_{max} (nm) (log ε) = 620 (7.7), 567 (2.4), 399 (3).

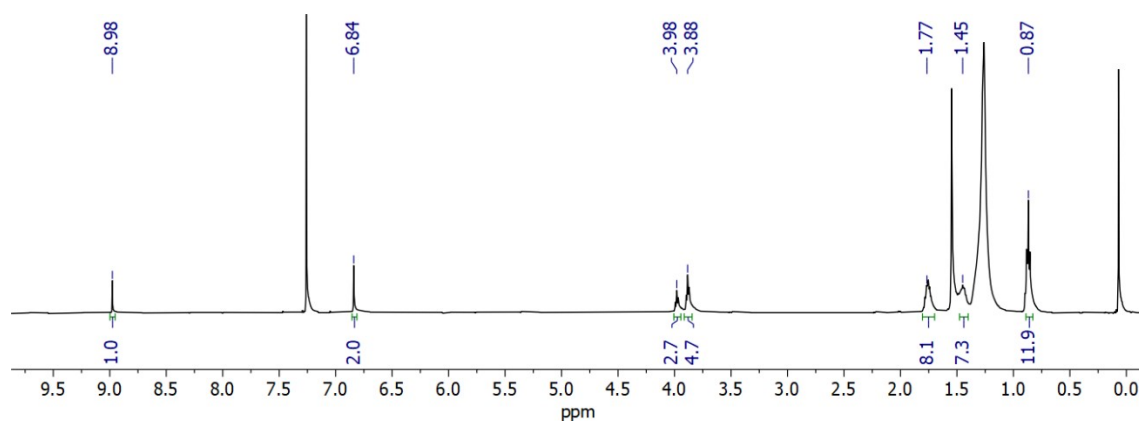


Figure S2.1. ¹H-NMR spectrum (CDCl₃) of SubPc 2

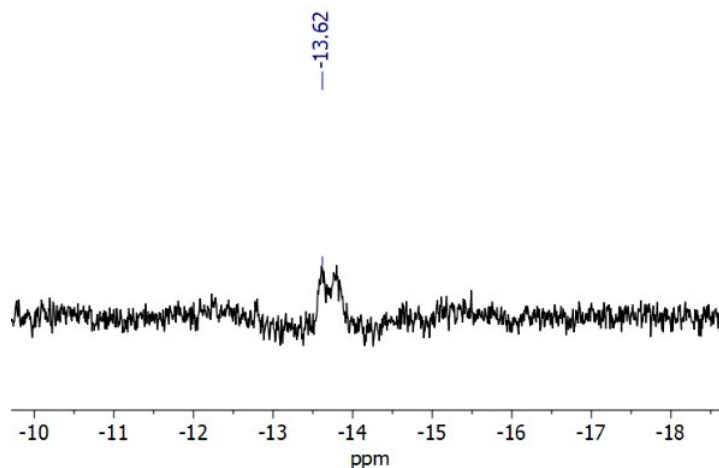


Figure S2.2. ¹¹B-NMR spectrum (CDCl₃) of SubPc 2

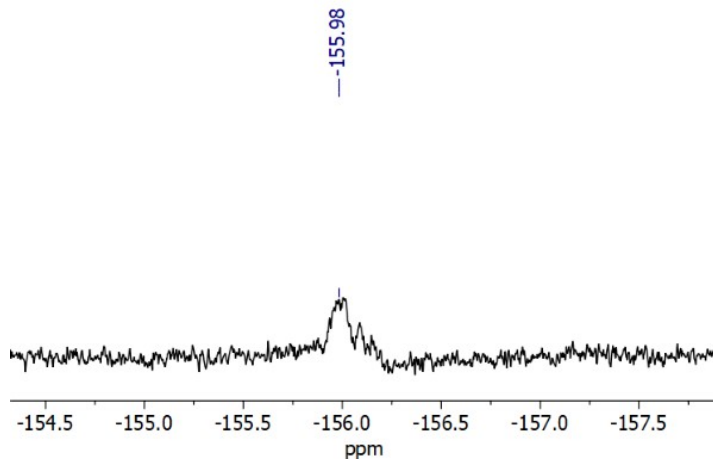
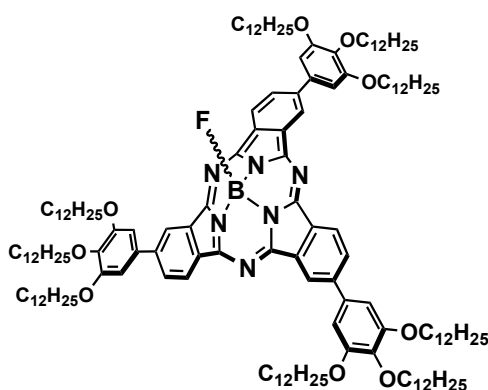


Figure S2.3. ^{19}F -NMR spectrum (CDCl_3) of **SubPc 2**

SubPc 3



In a 25 mL Schlenk flask, equipped with a magnetic stirrer, **Bpin₃SubPc-F** (20 mg, 0.025 mmol), $\text{PdCl}_2(\text{dppf})$ (4.5 mg, 0.005 mmol), Cs_2CO_3 (48.9 mg, 0.15 mmol), and 5-bromo-1,2,3-tris(dodecyloxy)benzene (78.2 mg, 0.15 mmol) were placed under argon atmosphere. Then, 2.0 mL of THF, which were deoxygenated via three freeze-pump-thaw cycles, were added and the resulting mixture was stirred at 60 °C for 4 h. After that, the crude was dissolved in DCM and passed through a short celite plug. The solvent was removed by vacuum distillation and the resulting dark purple solid was purified by column chromatography on silica gel using DCM/heptane 2:1. Upon recrystallization from methanol, **SubPc 3** was obtained as a purple viscous solid (43 mg, 0.019 mmol). Overall yield: 73%.

Mp = 123–126 °C; $^1\text{H-NMR}$ (300 MHz, CDCl_3): δ (ppm) = 9.05 (s, 3H), 8.90 (d, J = 8.3, 3H), 8.14 (d, J = 8.3, 3H), 7.04 (s, 6H), 4.15 (t, J = 6.3 Hz, 12H), 4.06 (t, J = 6.3 Hz, 6H), 1.90–1.79 (m, 18H), 1.34–1.22 (m, 162H), 0.87 (t, J = 5.7 Hz, 27H); $^{13}\text{C-NMR}$ (75.5 MHz, CDCl_3): 152.7, 150.0, 142.6, 137.9, 134.6, 130.8, 128.5, 119.3, 105.6, 95.9, 72.7, 68.5, 30.9, 30.9, 29.9, 29.4, 28.8, 28.6, 28.7, 28.7, 28.7, 28.5, 28.5, 28.4, 28.4, 25.2, 21.7, 13.1; $^{11}\text{B-NMR}$ (160.5 MHz, CDCl_3): δ (ppm) = 14.0 (d, J = 29.5 Hz, 1B; B–F); $^{19}\text{F-NMR}$ (470 MHz, CDCl_3): δ (ppm) = –156.7 (m, 1F; B–F); **MS** (MALDI-TOF, DCTB): m/z = 2300.8 $[\text{M}]^+$; **HRLSI-MS** (DCTB + PPGNa 5000): m/z Calculated for $[\text{C}_{150}\text{H}_{240}\text{BFN}_6\text{O}_9]$: 2300.8624, Found: 2300.8610. **UV-vis** (CHCl_3): λ_{max} (nm) ($\log \epsilon$) = 583 (4.9), 534 (1.6), 365 (1.5).

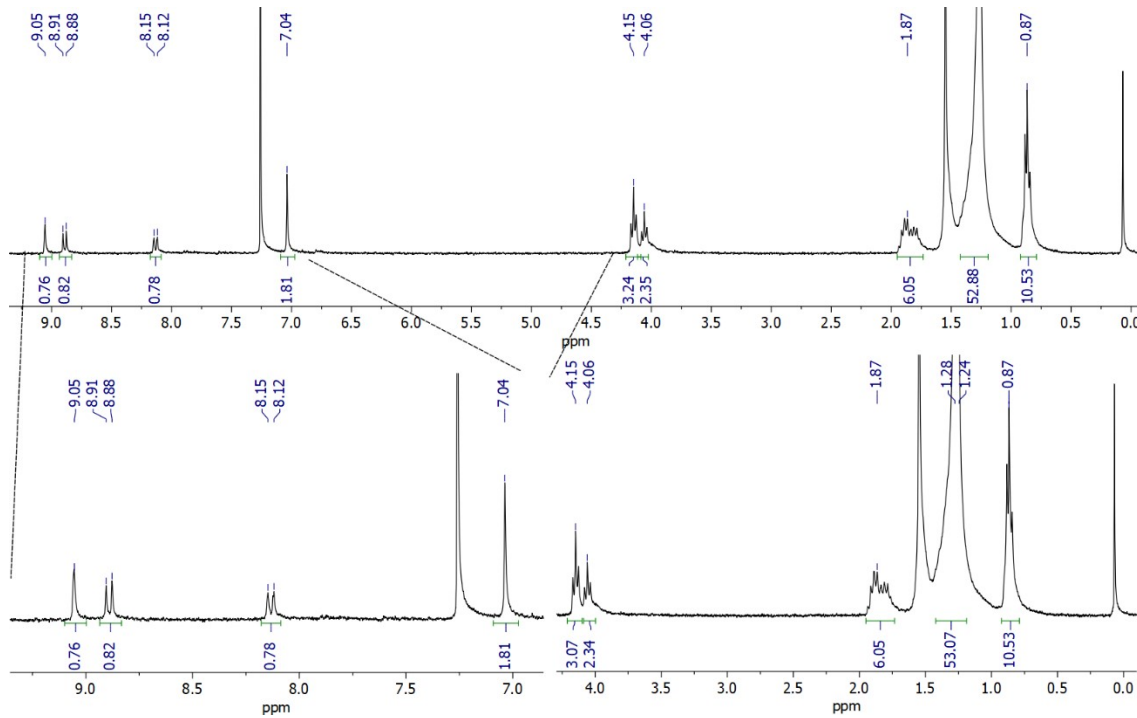


Figure S2.4. $^1\text{H-NMR}$ spectrum (CDCl_3) of SubPc 3

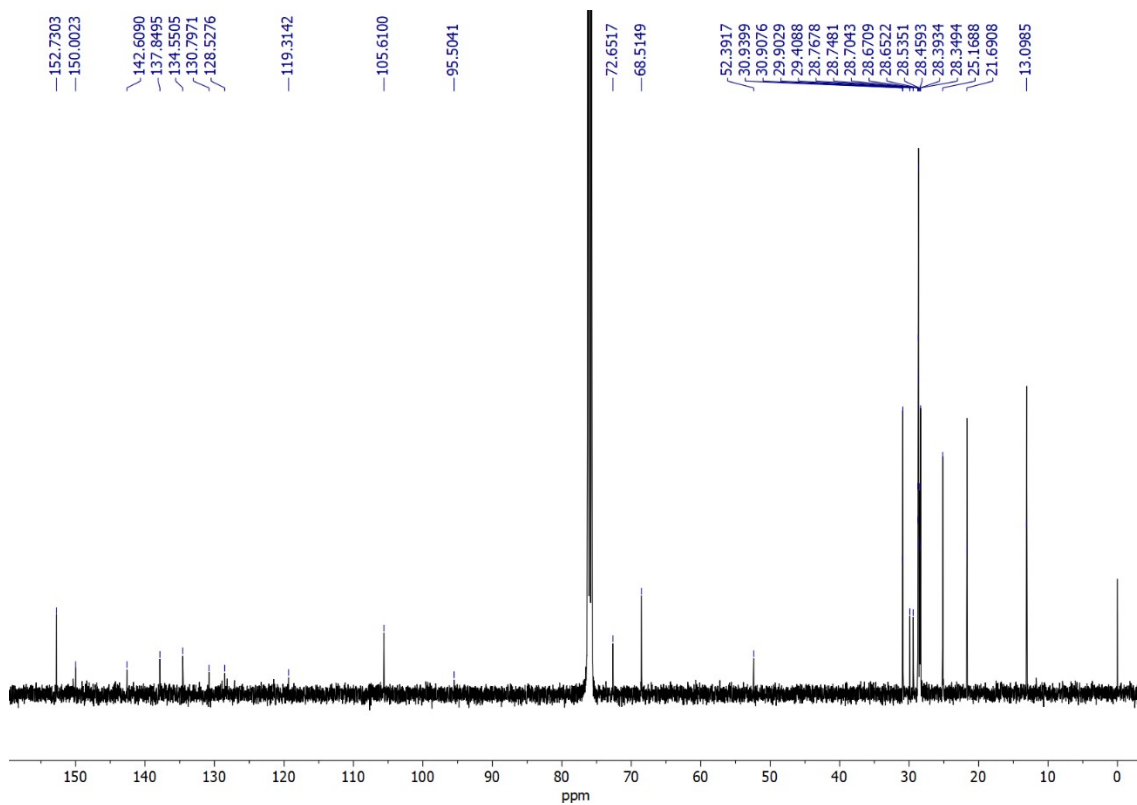


Figure S2.5. $^{13}\text{C-NMR}$ spectrum (CDCl_3) of SubPc 3

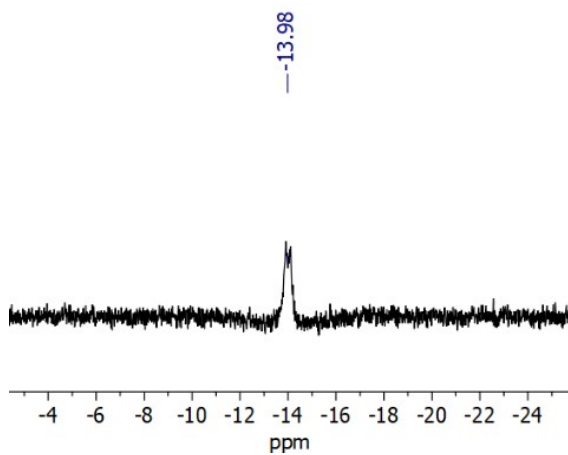


Figure S2.6. ^{11}B -NMR spectrum (CDCl_3) of SubPc 3

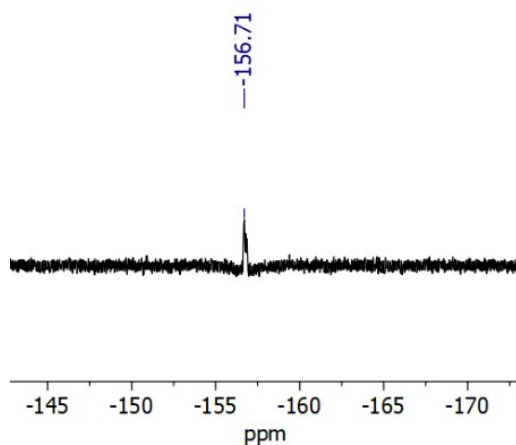


Figure S2.7. ^{19}F -NMR spectrum (CDCl_3) of SubPc 3

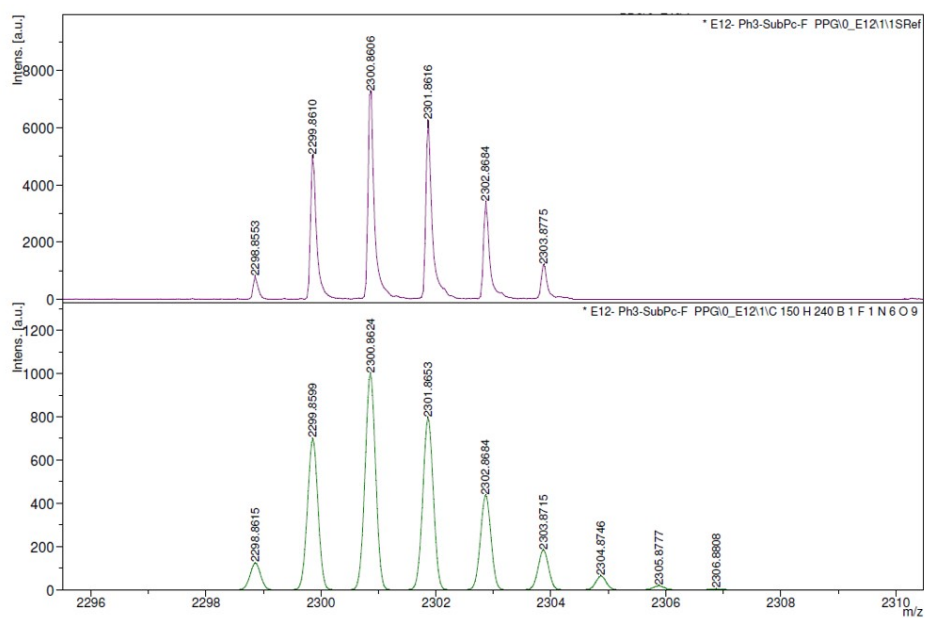


Figure S2.8. MALDI-TOF mass spectrum of SubPc 3

3. Additional liquid crystal characterization

Techniques

Liquid crystal behavior was examined by polarizing optical microscopy using a polarizing optical microscope Olympus BX51 equipped with an Olympus DP152 digital camera and connected to a Linkam THMS600 hot stage and a Linkam TMS94 controller. Transition temperatures and enthalpies were obtained by differential scanning calorimetry with DSC TA instruments Q20 at heating and cooling rates of 10 °C min⁻¹. The apparatus was previously calibrated with indium (156.6 °C, 28.71 J g⁻¹). Powder X-ray experiments were performed in a Pinhole diffractometer (Anton Paar) operating with a point focused Ni-filtered Cu-K α beam ($\lambda = 1.5418 \text{ \AA}$). The samples were held in Lindemann glass capillaries (0.9 mm diameter) and heated with a variable-temperature attachment. The diffraction patterns were collected on photographic films. X-ray diffraction diagrams in Figure SI6 were recorded using a Stoe Stadivari goniometer equipped with a Genix3D microfocuss generator (Xenocs) and a Dectris Pilatus 100K detector. Temperature control was achieved using a nitrogen-gas Cryostream controller (Oxford Cryosystems) allowing for a temperature control of about 0.1 °C. Lindemann capillaries of diameter 0.6 mm were utilized. Monochromatic Cu-K α radiation ($\lambda = 1.5418 \text{ \AA}$) was used.

POM

SubPc 1M/P

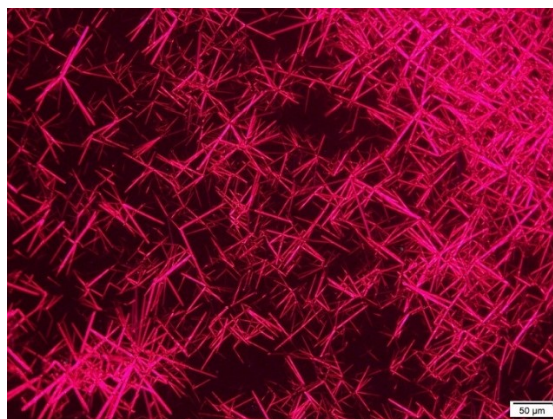
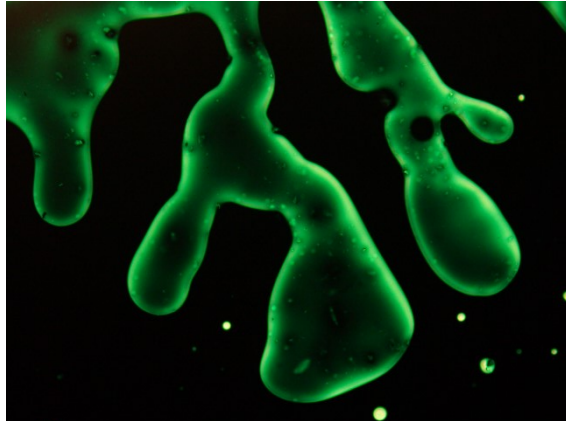


Figure S3.1. POM photograph of the crystallization process of **SubPc 1M** at 108 °C on cooling from the isotropic liquid at 10 °C/min. Similar images are obtained for **SubPc 1P**.



SubPc 2

Figure S3.2. POM photograph at 90 °C on cooling from the isotropic liquid and after mechanical stress by shearing.

DSC

SubPc 1*M/P*

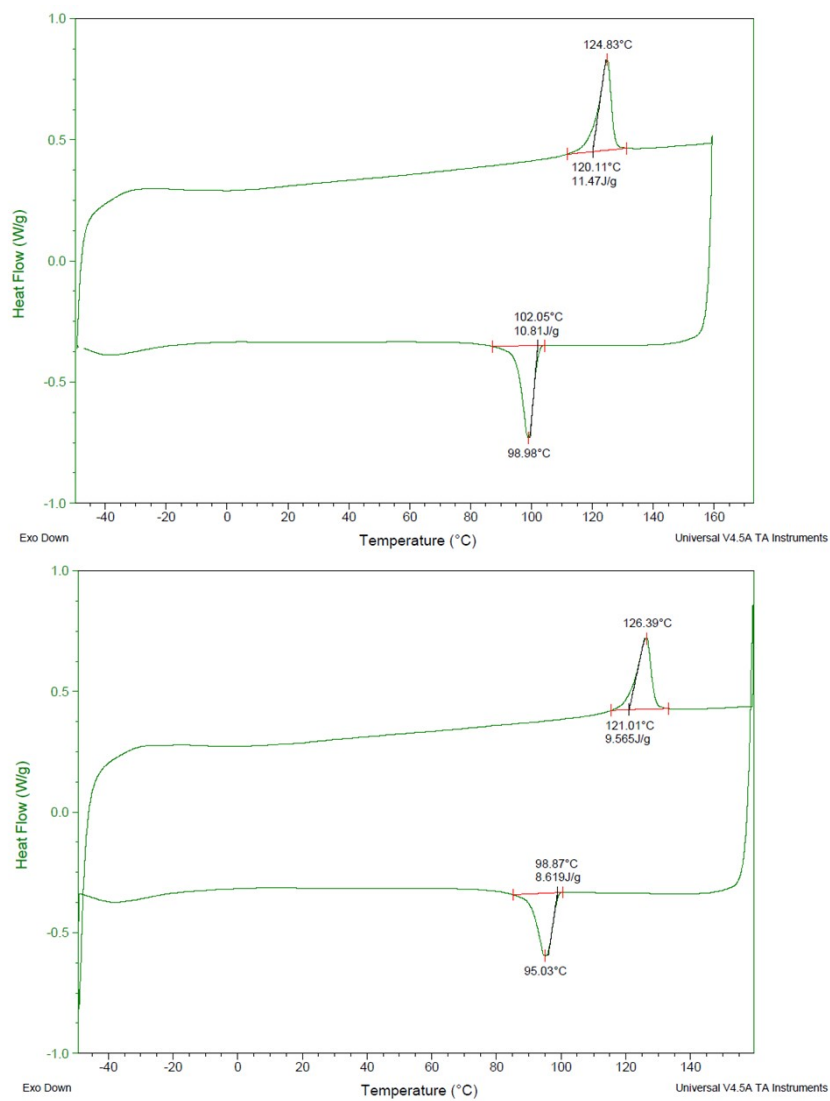


Figure S3.3. DSC thermograms corresponding to the second heating-cooling cycle recorded at 10 °C/min for both enantiomers of **SubPc 1** (top: *M*, bottom: *P*)

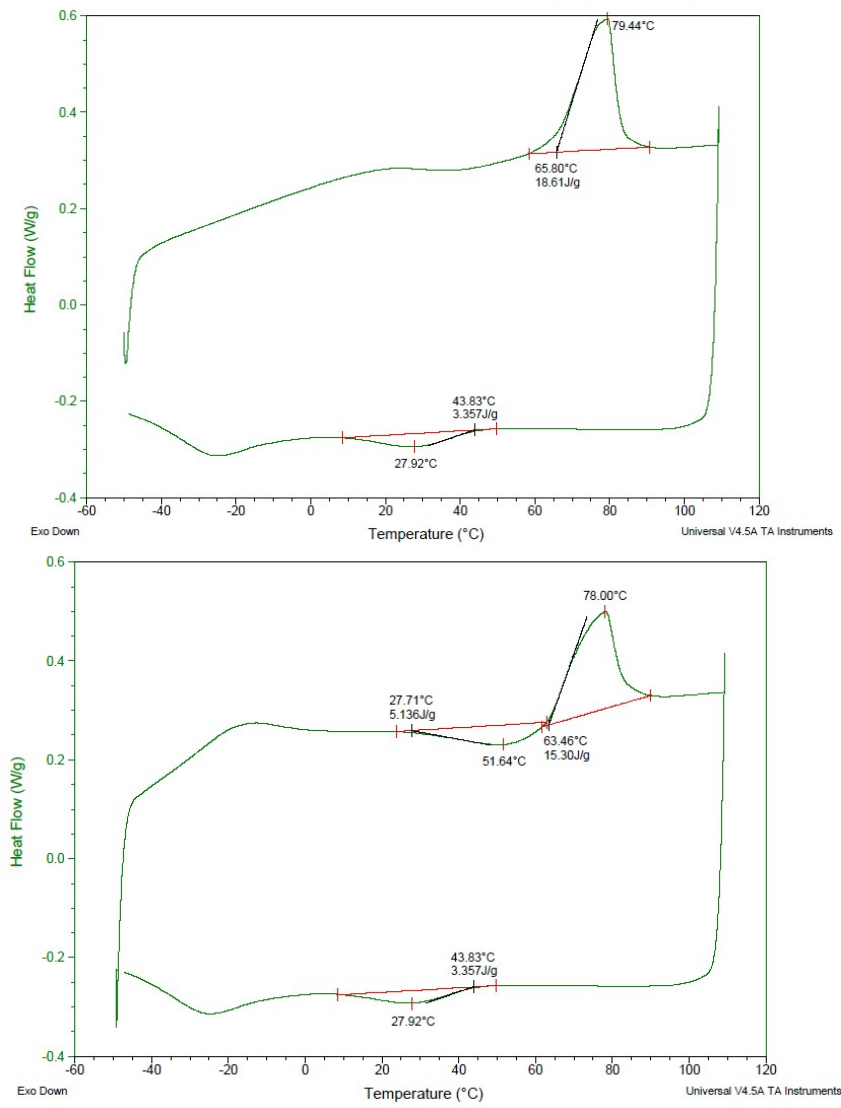


Figure S3.4. DSC thermograms corresponding to the first (left) and second (right) heating-cooling cycle recorded at 10 °C/min for **SubPc 2**.

SubPc 3

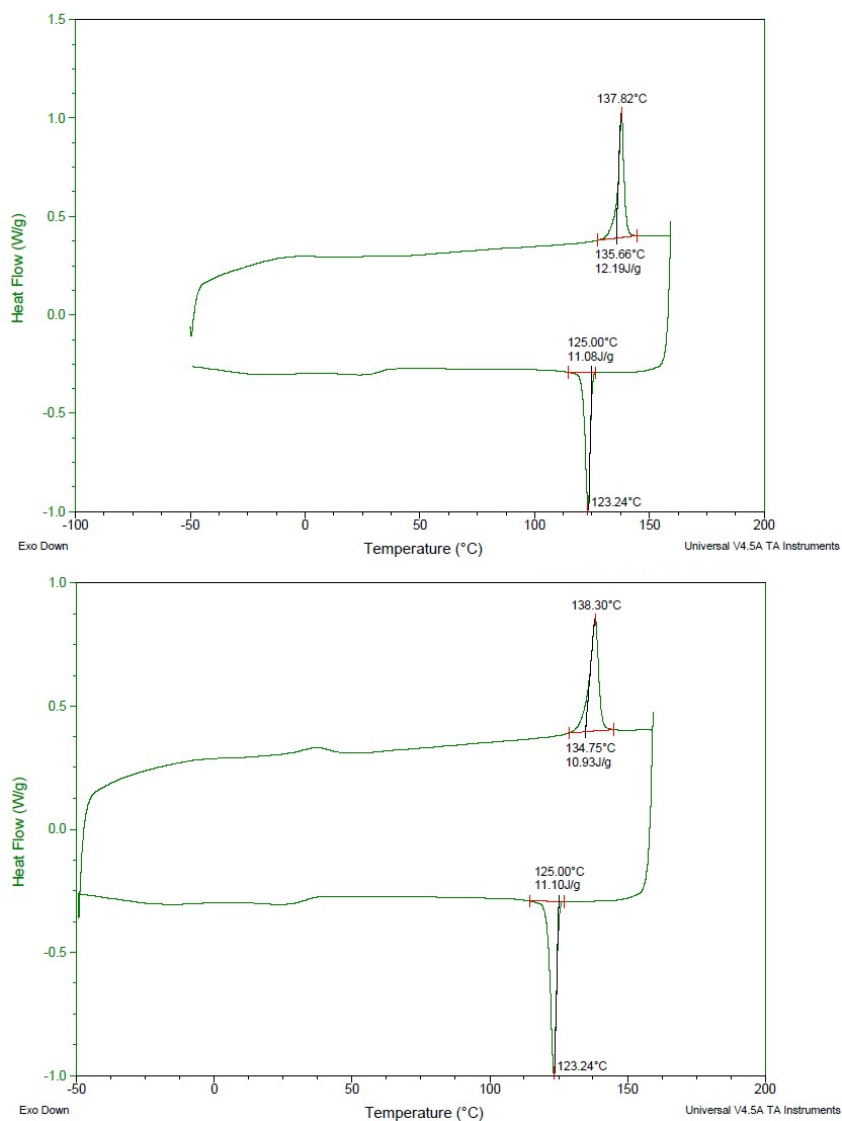


Figure S3.5. DSC thermograms corresponding to the first (top) and second (bottom) heating-cooling cycle recorded at 10 °C/min for **SubPc 3**.

SubPc 4

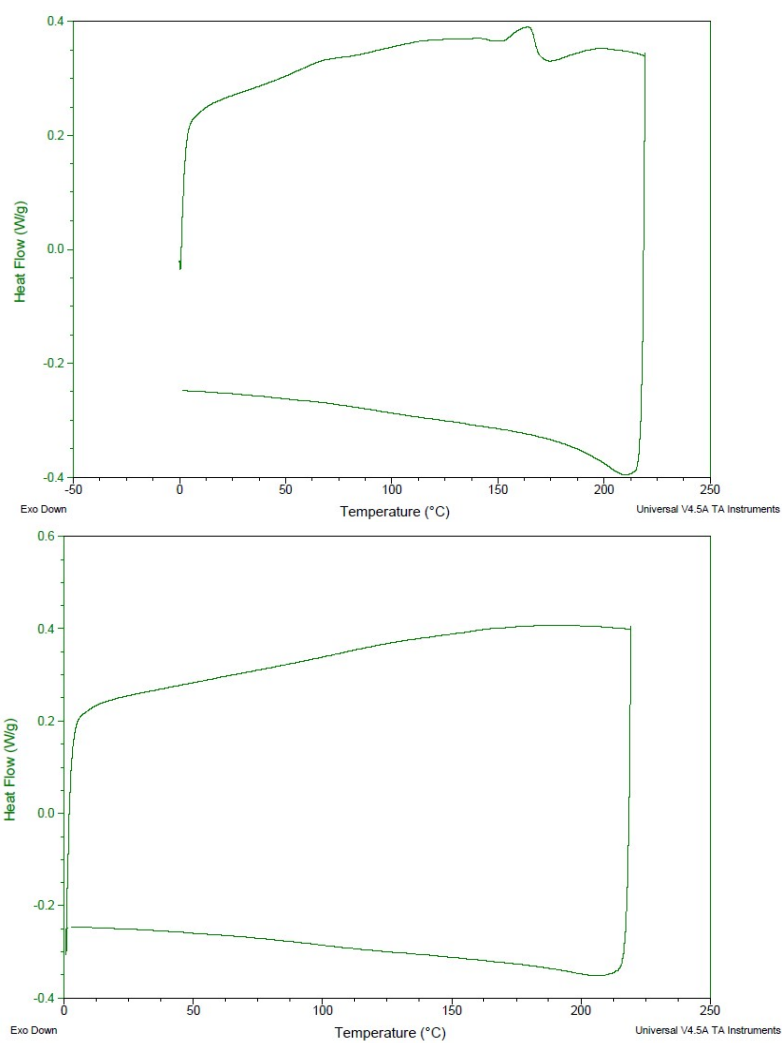


Figure S3.6. DSC thermograms corresponding to the first (top) and second (bottom) heating-cooling cycle recorded at 10 °C/min for **SubPc 4**.

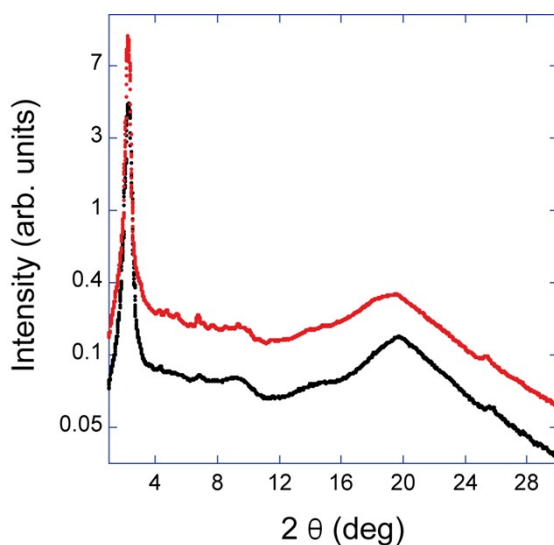


Figure S3.7. XRD pattern recorded for **SubPc 1M** at room temperature for the pristine sample (black) and after slow cooling from the isotropic liquid (red). The same pattern is observed for **SubPc 1P**

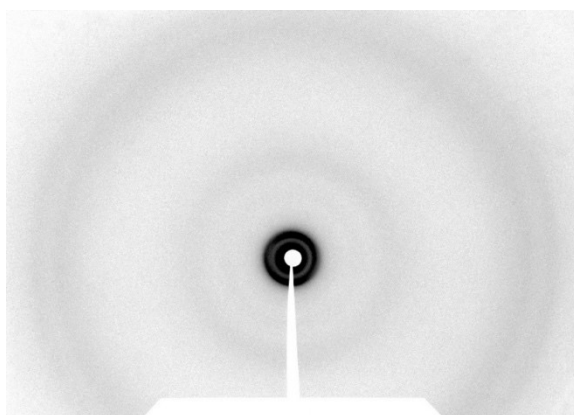


Figure S3.8. XRD diffractogram of **SubPc 2**, recorded in the pristine sample at a distance of 120mm.

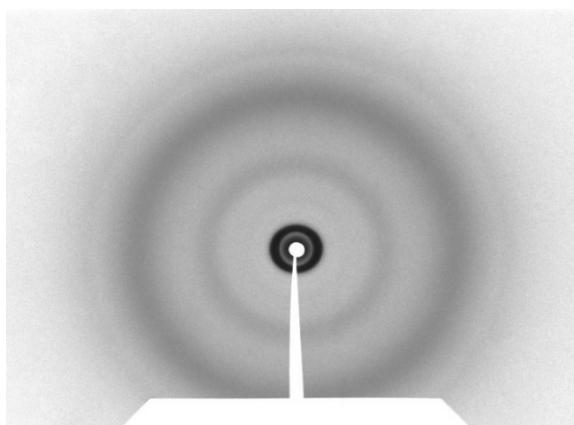


Figure S3.9. XRD diffractogram of **SubPc 3**, recorded in the pristine sample at a distance of 80mm.

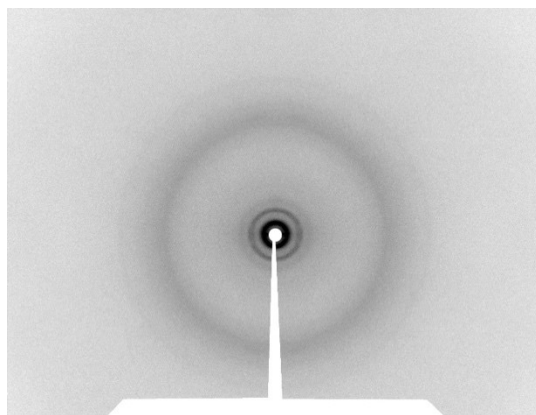


Figure S3.10. XRD diffractogram of **SubPc 4**, recorded in the pristine sample at a distance of 60 mm.

4. Theoretical calculations details

All reported structures were optimized at the GFN2-xTB level⁶ in the gas phase. Dimeric structures were also optimized by DFT to assess the discrepancies with the above-mentioned method. The DFT calculations were conducted using the B3LYP functional⁷ and the standard 6-31G(d) basis set. All of the calculations were carried out using the methods implemented in the Gaussian 16 package.⁸ As the DFT calculations proved concordant with those optimized at the GFN2-xTB level similar results, we decided to complete the study with GFN2-xTB in order to reduce computational costs.

5. References

- [1] N. R. Babij, E. O. McCusker, G. T. Whiteker, B. Canturk, N. Choy, L. C. Creemer, C. V. D. Amicis, N. M. Hewlett, P. L. Johnson, J. A. Knobelsdorf, F. Li, B. A. Lorsbach, B. M. Nugent, S. J. Ryan, M. R. Smith and Q. Yang, *Org. Process Res. Dev.* 2016, 20, 661.
- [2] J. Guilleme, J. Arago, E. Orti, E. Caverio, T. Sierra, J. Ortega, C. L. Folcia, J. Etxebarria, D. Gonzalez-Rodriguez and T. Torres, *J. Mater. Chem. C*, 2015, 3, 985–989.
- [3] J. Labella, E. López-Serrano, D. Aranda, M. J. Mayoral, E. Ortí and T. Torres, *Chem. Sci.*, 2024, 15, 13760–13767.
- [4] M. Obłozza, Ł. Łapok, J. Solarzski, T. Pedzinski, M. Nowakowska. *Chem. Eur. J.* 2018, 24, 17080 – 17090.
- [5] M-Gómez-Gómez, J. Labella, T. Torres. *Chem. Eur. J.* 2023, 29, e202301782.
- [6] C. Bannwarth, S. Ehlert, S. Grimme, *J. Chem. Theory Comput.* 2019, 15, 1652–1671.
- [7] (a) C. Lee, W. Yang, R. G. Parr, *Phys. Rev. B* 1988, 37, 785–789. (b) A. D. Becke, *J. Chem. Phys.* 1993, 98, 5648. (c) W. Kohn, A. D. Becke, R. G. Parr, *J. Phys. Chem.* 1996, 100, 12974–12980.
- [8] Gaussian 16, Revision C.01; Frisch, M. J.; Trucks, G. W.; Schlegel, H. B.; Scuseria, G. E.; Robb, M. A.; Cheeseman, J. R.; Scalmani, G.; Barone, V.; Petersson, G. A.; Nakatsuji, H.; Li, X.; Caricato, M.; Marenich, A. V.; Bloino, J.; Janesko, B. G.; Gomperts, R.; Mennucci, B.; Hratchian, H. P.; Ortiz, J. V.; Izmaylov, A. F.; Sonnenberg, J. L.; Williams-Young, D.; Ding, F.; Lipparini, F.; Egidi, F.; Goings, J.; Peng, B.; Petrone, A.; Henderson, T.; Ranasinghe, D.; Zakrzewski, V. G.; Gao, J.; Rega, N.; Zheng, G.; Liang, W.; Hada, M.; Ehara, M.; Toyota, K.; Fukuda, R.; Hasegawa, J.; Ishida, M.; Nakajima, T.; Honda, Y.; Kitao, O.; Nakai, H.; Vreven, T.; Throssell, K.; Montgomery, J. A., Jr.; Peralta, J. E.; Ogliaro, F.; Bearpark, M. J.; Heyd, J. J.; Brothers, E. N.; Kudin, K. N.; Staroverov, V. N.; Keith, T. A.; Kobayashi, R.; Normand, J.; Raghavachari, K.; Rendell, A. P.; Burant, J. C.; Iyengar, S. S.; Tomasi, J.; Cossi, M.; Millam, J. M.; Klene, M.; Adamo, C.; Cammi, R.; Ochterski, J. W.; Martin, R. L.; Morokuma, K.; Farkas, O.; Foresman, J. B.; Fox, D. J. Gaussian, Inc., Wallingford CT, 2016